JOURNAL OF VIROLOGY, Mar. 2005, p. 3127–3138 Vol. 79, No. 5
0022-538X/05/$08.00+0 doi:10.1128/JVI.79.5.3127–3138.2005

The Latency-Associated Nuclear Antigen of Rhesus Monkey Rhadinovirus Inhibits Viral Replication through Repression of Orf50/Rta Transcriptional Activation

Scott M. DeWire[1] and Blossom Damania[1,2]*

Curriculum in Genetics and Molecular Biology[1] and Department of Microbiology and Immunology and Lineberger Comprehensive Cancer Center,[2] University of North Carolina at Chapel Hill, Chapel Hill, North Carolina

Received 28 June 2004/Accepted 29 September 2004

Rhesus monkey rhadinovirus (RRV) is a gamma-2-herpesvirus that is closely related to Kaposi's sarcoma-associated herpesvirus/human herpesvirus-8. We have previously reported that the transcript for RRV latency-associated nuclear antigen (R-LANA) is expressed during lytic replication in rhesus fibroblasts. In this article, we report the development of a latent culture system for RRV and show that mRNA specific for R-LANA is expressed during latency as well. We have characterized the R-LANA protein and demonstrate that it exhibits a nuclear speckled localization and possesses the ability to homodimerize. When expressed in rhesus fibroblasts, R-LANA can inhibit RRV lytic replication in vitro. We have investigated the mechanism behind this inhibition and find that, while R-LANA itself has very little effect on lytic promoters, it can dramatically decrease the transactivation function of RRV Orf50 (Rta), which is the major viral transcription factor. We further show that the mechanism for this repression involves the recruitment of histone deacetylase complexes (HDACs), because R-LANA's ability to repress Orf50 transactivation is completely reversed by the addition of the HDAC inhibitor trichostatin A (TSA). We also report that TSA alone can significantly reactivate RRV from latently infected cells. We propose that the repressive effects of R-LANA on RRV Orf50 transactivation serve to downregulate the transcription of early genes at late times during the lytic cycle and also help to maintain viral latency by preventing viral reactivation.

Kaposi's sarcoma-associated herpesvirus (KSHV) is the etiologic agent of Kaposi's sarcoma, primary effusion lymphoma (PEL), and multicentric Castleman's disease (7, 8, 57). Rhesus monkey rhadinovirus (RRV) was first isolated from rhesus macaques in 1997 at the New England Primate Research Center (13). A second isolate was also identified at the Oregon Regional Primate Research Center, and the genomes of both these isolates have been fully sequenced, revealing high relatedness sequence to KSHV (1, 56). RRV serves as a useful animal model system to study the life cycle of KSHV in vivo and in vitro. This is because KSHV cannot persistently infect mice or rhesus macaques (18, 49) and because only 20 to 30% of latently infected PEL cells can be reactivated with 12-*O*-tetradecanoylphorbol-13-acetate (TPA) (50). Replication assays using de novo infection of endothelial cells with KSHV have been developed, but these assays are hampered by the inability to obtain high viral titers or to passage the virus over extended periods of time (16, 34, 48, 51).

In contrast, RRV infection of rhesus fibroblasts (RhFs) yields high titers of virus ($\sim 10^6$ PFU/ml), which greatly facilitates the analysis of the RRV lytic life cycle and the construction of recombinant viruses. In addition, naive rhesus macaques can be experimentally infected with RRV (40, 61). Our laboratory previously demonstrated that the kinetics of RRV gene expression during de novo infection of RhFs closely resembles that of KSHV reactivation (14). We identified the expression of the RRV Orf50, R8, and R8.1 spliced transcripts during lytic replication (14) and characterized the transcriptional function of the RRV Orf50 protein (12, 14). Further, we also reported the construction of an RRV-green fluorescent protein (GFP) recombinant virus and assays to measure viral replication (15). Other macaque rhadinoviruses (reviewed in reference 11) have been discovered by amplifying short stretches of the DNA polymerase gene (54).

One of the most intensely studied KSHV proteins is the latency-associated nuclear antigen (LANA) (reviewed in reference 31). KSHV LANA functions in a mechanical capacity during viral latency (4), tethering the viral episome to the host chromosome and thus ensuring its segregation during mitosis (9, 10, 23, 24, 26). A number of other proteins involved in this bridging process have since been identified (32). Further, KSHV LANA has been shown to play many different roles within the latently infected cell. KSHV LANA can promote cell survival and prevent apoptosis by interacting with the tumor suppressor protein p53 (21). LANA can also regulate the Rb-E2F pathway and cooperate with h-Ras to promote cellular transformation (46) and has been shown to stimulate S-phase entry by stabilizing beta-catenin through a novel mechanism involving the cell cycle-dependent nuclear accumulation of its inhibitor, glycogen synthase kinase 3β (22). Further, KSHV LANA can interact with the RING3 protein, an interaction which results in its own phosphorylation (41, 45). An important function of LANA is its role as a transcriptional modulator. LANA can activate both viral and cellular promoters, including the LANA promoter itself (28); E2F-responsive promoters;

* Corresponding author. Mailing address: Lineberger Comprehensive Cancer Center, CB #7295, University of North Carolina, Chapel Hill, NC 27599. Phone: (919) 843-6011. Fax: (919) 966-9673. E-mail: damania@med.unc.edu.

and the interleukin-6 (2), c-JUN (3), and human telomerase reverse transcriptase promoters (30). LANA has also been shown to function as a repressor of transcription (55), acting at least partially though the mSIN3 complex (33).

While KSHV LANA has been the subject of intense research, the properties of RRV LANA (R-LANA) have not been investigated thus far. At the amino acid level, R-LANA shows a significant degree of homology to KSHV LANA. However, this homology is limited to the N- and C-terminal ends of the protein. R-LANA is 448 amino acids in length, while the size of KSHV LANA ranges from 1,089 to 1,162 amino acids, due to the variable-length internal acidic repeat domain, a region that is completely absent from R-LANA. We have previously demonstrated that R-LANA is transcribed during RRV lytic replication (14), while KSHV LANA mRNA has been reported to be either marginally upregulated (27, 43) or uninduced (20, 59) upon reactivation of latently infected cell lines. Our prior observation regarding R-LANA transcription during RRV lytic replication prompted us to determine the role of R-LANA in the RRV life cycle.

Here, we describe the initial characterization of R-LANA. We have mapped the transcription start site using 5′ rapid amplification of cDNA ends (RACE), as well as the subcellular localization, self-association, and transcriptional properties of the R-LANA protein itself. We have found that expression of R-LANA during lytic infection results in an inhibition of RRV replication. Further, we demonstrate that the mechanism of this inhibition is through R-LANA-mediated inhibition of the transactivation function of the RRV Orf50/Rta protein. R-LANA's ability to repress the RRV lytic cycle may help downregulate the transcription of early genes at late times during lytic replication and may also help to maintain the latent state of the viral life cycle by suppressing viral reactivation.

MATERIALS AND METHODS

Cell culture. RhFs were immortalized as previously described (14). RhF, 293, and 293-RRV-GFP cells were maintained at 37°C and 5% CO_2 in Dulbecco's modified eagle medium H with Gluta-max supplemented with 10% fetal bovine serum. BJAB and BJAB-RRV-GFP cells were maintained in RPMI 1640 supplemented with 10% fetal bovine serum. Construction of RRV-GFP has been previously described (15).

Establishment of BJAB-RRV-GFP and 293-RRV-GFP cells. BJAB or 293 cells were infected with RRV-GFP at a multiplicity of infection (MOI) of >1 in the presence of 4 μg of Polybrene (Sigma; 52495)/ml for 1 h. The virus inoculum was removed, and cells were resuspended in appropriate complete media plus 500 μM ganciclovir (GCV). BJAB cells were subjected to flow cytometry. Briefly, the RRV-GFP-infected BJAB cells were sorted on a modular flow cytometer (Cytomation Inc.) based on GFP expression. The top 5% of the most highly fluorescing cells were collected and passaged in tissue culture to establish the BJAB-RRV-GFP latent cell line. After sorting, both BJAB-RRV-GFP and 293-RRV-GFP cells were passaged for 4 weeks in GCV. After 4 weeks, GCV was removed from the media, and cells were then passaged in regular complete media.

Plasmids. R-LANA was amplified by PCR from RRV H26-95 viral DNA (1) with primers complementary to the genomic open reading frame. The resulting PCR product was cloned into the Spe1 and EcoR1 sites of pEF1-myc-HisA (Invitrogen). The 5′ primers included either an AU1 (Covance) or FLAG (Sigma) epitope sequence. Red fluorescent R-LANA fusion constructs were created by cloning the R-LANA coding sequence into the pdsRed-N1 vector (Clontech) at BamH1 and Xho1 sites with primers 1 (5′-CTCGAGATGTGGGGCAGCCGGCAACAT-3′) and 2 (5′-GGATCCCCGTGCTGAATTGGCAGTCCTCTG-3′). R-LANA was fused to the N terminus of red fluorescent protein (RFP). R-$LANA_{1-25}$–RFP was made with primers 1 and 3 (5′-GGATCCCCTCCGCAATGTCCCCTGCAGGAACT-3′). R-$LANA_{297-448}$–RFP was made with primers 4 (5′-CTCGAGATGGAGGAGCGGCAGCAGCAACCG-3′) and 2. R-$LANA_{46-448}$–RFP was made with primers 5 (5′-CTCGAGATGGCCAGCCTGCCTGCACCCC-3′) and 2. The fibrillarin-GFP plasmid was kindly proved by M. Olson (19). The pcDNA3-RRV Orf50 expression plasmid has been described previously (14).

5′ and 3′ RACE. mRNA was harvested from RRV-infected RhFs at 72 h postinfection or from unstimulated 293-RRV latent cultures with the RNEasy kit (QIAGEN) and was subsequently treated with RQ-DNase (Promega). cDNA was reverse transcribed with the Smart RACE system (Clontech, BD), and R-LANA-specific messages were amplified with the following primers: 5′-CGATACTATGCCGGAACGATGTTG-3′ (5′ RACE) and 5′-GCCGGACGCACCTGGCAGTCCCGTCAT-3′ (3′ RACE). PCR products were cloned into pCR2.1-Topo (Invitrogen) and sequenced.

RT-PCR and Northern hybridization. Total RNA was harvested from 293-RRV-GFP cells with the RNEasy kit (QIAGEN) according to the manufacturer's protocol. For Northern hybridization, 4 μg of total RNA was added per lane and hybridization was performed by a previously described protocol (14). An R-LANA DNA probe was made with RRV 26–95 (nucleotides [nt] 118646 to 119992) viral DNA. RNA used for reverse transcriptase PCR (RT-PCR) was treated with RQ-DNase1 (Promega) and reverse transcribed with the Promega reverse transcription system. PCR was performed with Platinum *Pfx* polymerase (Invitrogen) with an annealing temperature of 58°C and the following primers: Orf71, 5′-CAACCAGTCACCCACCTTTT-3′ and 5′-TGCAGCAGGTCACTTAAAACC-3′; Orf72, 5′-CCAGGTGGTGGAGTCTGTTC-3′ and 5′-GCACCGAGGCTAAACAGC-3′; Orf73, 5′-TCACGGTGTTCTGTCAAAGC-3′ and 5′-CTATGCTGGCCTGGAAGTG-3′.

Coimmunoprecipitations and Western blots. 293 cells on 10-cm dishes were transfected with Superfect reagent (QIAGEN) with either 10 μg of DNA for each construct (for coimmunoprecipitations) or 15 μg of DNA for a single construct. Forty-eight hours posttransfection, the cells were harvested with radioimmunoprecipitation assay lysis buffer (14) for Western blots or NP-40 lysis buffer (150 mM NaCl, 0.1% NP-40, 50 mM Tris-Cl [pH 8.0]) for immunoprecipitations. Antibodies used for immunoprecipitations and Western blots included monoclonal anti-AU1 (Covance; MMS-130R), anti-AU1-horseradish peroxidase (HRP) (Bethyl; A190-124P), monoclonal anti-FLAG (Sigma; A-8592), FLAG-HRP (Sigma; F-3040), monoclonal anti-GFP (Clontech; 8362-1), and peptide GFP-HRP (Clontech; 8369-1). The secondary antibody used for detection of R-LANA–GFP was sheep anti-mouse antibody conjugated to HRP (Cappel/ICN; 55569). For coimmunoprecipitations, lysates were precleared with protein A/G beads (Santa Cruz Biotechnology; A0704) and incubated with a primary monoclonal antibody for 4 h at 4°C. Protein A/G beads were then added for 4 h at 4°C. Complexes were centrifuged at 10,000 × *g* for 6 min and washed three times with NP-40 lysis buffer prior to denaturation in sodium dodecyl sulfate-polyacrylamide gel electrophoresis (SDS-PAGE) loading buffer at 70°C for 5 min.

In vitro dephosphorylation assay. 293 cells in three 10-cm dishes were transfected with pEF-R-$LANA_{FLAG}$. Forty-eight hours posttransfection, cells were harvested and lysed in NP-40 lysis buffer. Immunoprecipitations were performed as described above with the monoclonal anti-FLAG antibody. After three washes with NP-40 lysis buffer, agarose beads were resuspended in 100 μl of New England Biolabs no. 3 buffer (100 mM NaCl, 50 mM Tris-Cl, 10 mM $MgCl_2$, 1 mM dithiothreitol [pH 7.9]). The resuspended beads were divided equally into two fractions. Three microliters of calf intestine phosphatase (CIP) (NEB; M0290S) was added to one fraction and 3 μl of phosphate-buffered saline was added to the other. Reaction mixtures were incubated at 37°C for 1 h. Beads were pelleted by centrifugation and washed once with NP-40. Bound proteins were eluted in SDS-PAGE lysis buffer and subjected to Western blotting as described above.

Cellular localization assay. LANA-RFP fusion proteins were transfected into RhF cells by electroporation (250 V, 500 μF), and cells were allowed to recover for 48 h. Cells were fixed on tissue culture chamber slides and treated with DAPI (4′,6′-diamidino-2-phenylindole) nuclear stain. Cells were visualized on a fluorescence microscope, and images were captured with the OpenLab software suite.

Viral infections. Equivalent numbers of RhFs were transfected with pEF-R-$LANA_{FLAG}$ or pEF expression plasmids by using the Amaxa Nucleofection system as described by the manufacturer (program U-23). Following transfection, cells were recovered in complete media for 24 h. RRV-GFP recombinant virus (15) was used to infect the transfected RhFs at an MOI greater than 1. Cell-free supernatants were harvested 72 h postinfection, and viral titer was determined by a plaque assay as previously described (15).

Viral genome immunoprecipitation assay. 293-RRV-GFP cells in 10-cm culture dishes were transfected with 15 μg of either pEF-R-$LANA_{FLAG}$, pEF, pdsRed-N1 (encoding RFP), or p-R-LANA-RFP and recovered in complete media for 72 h. Protein-DNA complexes were cross-linked with 270 μl of 37%

formaldehyde, and cells were washed twice with phosphate-buffered saline. Lysis was performed with 400 μl of an SDS lysis buffer (1% SDS, 10 mM EDTA, 50 mM Tris-HCl [pH 8.1]) and one freeze-thaw cycle. Lysates were diluted with 1 ml of chromatin immunoprecipitation dilution buffer (0.1% SDS, 1.1% Triton X-100, 1.2 mM EDTA, 16.7 mM Tris-HCl [pH 8.1], 167 mM NaCl), and 10 μl of antibody was added as follows: 10 μl of the FLAG monoclonal antibody (Sigma; F-3040) was added to the pEF- and pEF-R-LANA-transfected cell lysates, and 10 μl of the dsRed monoclonal antibody (Clontech, BD; 632392) was added to the dsRed-N1 and R-LANA–RFP lysates. Immunoprecipitation was performed on a nutator for 16 h at 4°C. Sixty microliters of a 50% (wt/vol) solution of protein A/G-agarose beads was added to each sample, along with 400 μg of sonicated salmon sperm DNA/ml. Samples were incubated for 2 h on a nutator at 4°C. Agarose beads were centrifuged at 2,000 × *g* for 2 min and washed with each of the following buffers for 5 min: (i) low-salt buffer (0.1% SDS, 1% Triton X-100, 2 mM EDTA, 20 mM Tris-HCl [pH 8.1], 150 mM NaCl), (ii) high-salt buffer (same as low-salt buffer but with 500 mm NaCl), (iii) LiCl buffer (0.25 M LiCl, 1% NP-40, 1% deoxycholate, 1 mM EDTA, 10 mM Tris-HCl [pH 8.1]), and (iv) TE (10 mM Tris-HCl, 1 mM EDTA [pH 8.0]) (two washes). Cross-links were reversed by addition of 20 μl of 5 M NaCl and incubation at 65°C for 4 h. DNA-protein complexes were then eluted from agarose beads with two 250-μl elution volumes of a 1% SDS–0.1 M $NaHCO_3$ solution. Eluates were analyzed for RRV genome content by either Southern hybridization with a GFP-specific probe or real-time quantitative PCR (QPCR), as previously described (15).

Luciferase reporter assays. 293 cells (10^5) were plated in each well of a 24-well plate. Twenty-four hours later (50 to 70% confluence) cells were transfected with Superfect reagent (QIAGEN), with a total of 5.5 μg of DNA per well (0.5 μg of luciferase-promoter reporter plasmid and 2.5 μg of each effector plasmid, i.e., pRF-R-LANA and pcDNA3-Orf50). The total amount of effector plasmid DNA transfected was always kept constant by normalizing with vector plasmid pEF or pcDNA3. Each transfection was performed in triplicate, and data shown are representative of at least three separate experiments. Forty-eight hours post-transfection, cells were lysed on the plate with the MPER reagent (Pierce) and analyzed for luciferase content as previously described (14). Where applicable, trichostatin A (TSA) (Sigma; T-8552) was added 18 h prior to harvest at 100 nM. An equivalent volume of ethanol was added to control samples.

Viral reactivation. BJAB-RRV and 293-RRV cells were treated with TPA (25 ng/ml), dimethyl sulfoxide (DMSO), TSA (Sigma; T-8552; 100 nM), or ethanol. Seventy-two hours posttreatment, cell-free supernatants from each population were visually inspected for intensity of GFP and also assayed for the presence of the RRV genome by real-time PCR.

RESULTS

Generation of a latent culture system for RRV. As a tool to study the latent phase of RRV, we sought to develop cell lines that latently harbor RRV. Using a RRV-GFP recombinant virus (15), we infected many different cell lines including 293-HEK, immortalized human umbilical vein endothelial cells (HUVEC) (60), HeLa cells, RhFs, and BJAB B cells with RRV-GFP. We assayed the infected cells for infectious virus using plaque assays as previously described (15). Although RRV-GFP could efficiently enter all of these cells, detectable virus was produced only from HUVEC and RhFs (Fig. 1B). To generate cell lines latently harboring RRV, we infected the 293-HEK and BJAB cells with RRV-GFP virus with or without Polybrene at an MOI of >1 (Fig. 1). While the infection efficiency of RRV-GFP in 293-HEK cells was extremely high, with nearly 100% of cells infected, only about 10% of BJAB cells expressed GFP following RRV-GFP infection. To obtain a pure population of RRV-GFP-infected BJAB cells, flow cytometry was performed to sort the most intensely green fluorescing cells and this population was subsequently passaged and amplified. Viral supernatants from these infected 293 and BJAB cells were harvested and examined by a plaque assay. As described above, no visible cytopathic effect was detected from either the infected BJAB or 293 cells, in contrast to the RhFs and HUVEC (Fig. 1B). The 293-RRV-GFP and BJAB-RRV-GFP cell lines were also passaged for 4 weeks in the presence of GCV, which, we have previously demonstrated, potently inhibits RRV replication (15). Survival of the GFP-positive 293 and BJAB infected cells in GCV-containing media indicated that RRV infection was latent, and the persistence of GFP-expressing cells was not a result of low-level lytic replication. After 4 weeks, the cells were passaged in media without GCV. TPA, when added directly to the media of these cells, was able to induce lytic replication, as measured by real-time QPCR (data not shown). This indicated that the BJAB-RRV-GFP and 293-RRV-GFP cells were latently infected but could be induced to lytic replication in a fashion similar to KSHV-infected cells. However, these two cell lines display a background of spontaneous lytic replication since we can detect a small percentage of extracellular viral genomes by real-time QPCR in the absence of TPA, although the PFU of infectious virus are rarely detectable in these cultures (Fig. 1B). We have

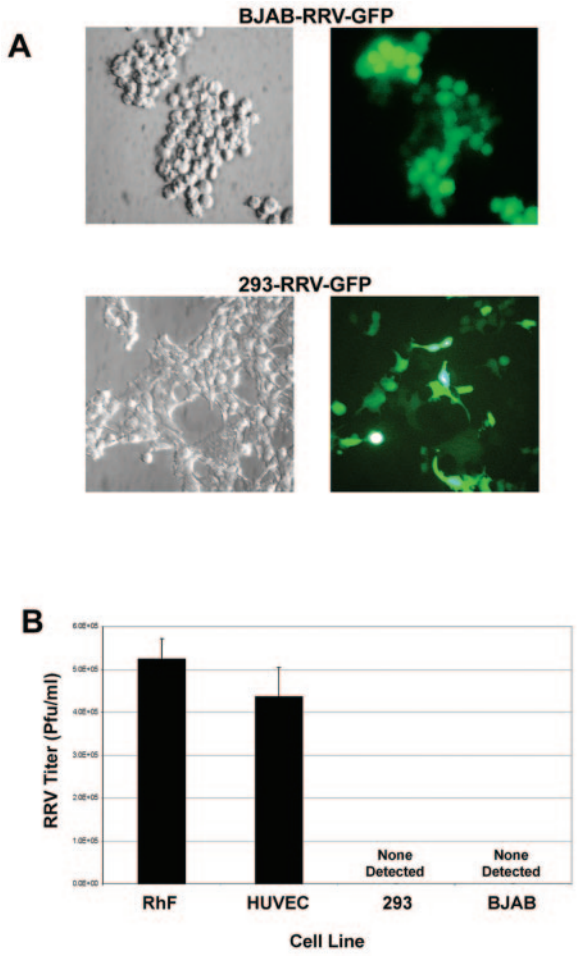

FIG. 1. Cell lines latently infected with RRV-GFP. (A) BJAB or 293 cells were infected with RRV-GFP and passaged for several weeks. The BJAB-RRV-GFP-positive cells were sorted and pooled by flow cytometry. Cell lines were passaged in GCV to confirm the persistence of latent infection. (B) RRV can undergo lytic replication in RhFs and HUVEC but not in 293 or BJAB cells. Cells were infected with RRV-GFP at an MOI of ≥1, and infections were carried out for 72 h. Cell-free supernatants were harvested, and viral infectivity was determined by plaque assay.

also observed that transient transfection of an RRV Orf50 expression plasmid into the BJAB-RRV-GFP cell line results in approximately fourfold reactivation of the viral lytic cycle, as measured by plaque assay (data not shown). We passaged both the 293-RRV-GFP and BJAB-RRV-GFP latently infected cell lines for over 3 months and observed that they still maintain their GFP positivity. However, we noticed a dramatic decrease in the reactivation induced by TPA after several weeks of passaging in culture. Thus, we conclude that the 293-RRV-GFP and BJAB-RRV-GFP cell lines are latently infected with RRV-GFP and can be used as tools to study RRV latency.

Identification of the R-LANA mRNA transcript during latency. We have previously reported the appearance of sense strand R-LANA transcripts during RRV lytic replication (14). To determine if R-LANA was expressed in the 293 and BJAB cell lines latently infected with RRV-GFP, mRNA was harvested and RT-PCR was performed with primers specific to R-LANA. Figure 2A shows that mRNA transcripts for R-LANA (Orf73), RRV Orf71 (vFlip), and RRV Orf72 (vCyc) were all expressed in the BJAB-RRV-GFP cells (Fig. 2A) and 293-RRV-GFP cells (data not shown). No products were observed in the lanes that did not contain reverse transcriptase (Fig. 2A, lane −RT). We have previously reported the transcription of these three RRV genes during the lytic cycle as a polycistronic transcript (14), similar to the situation in KSHV (17, 52). To confirm the RT-PCR results, Northern hybridization of RNA from 293-RRV-GFP cells was performed. Three R-LANA transcripts were detected (Fig. 2B) in the 293-RRV-GFP cells, indicating that R-LANA is expressed during RRV latency, similar to the situation in KSHV. The sizes of the three transcripts seen in the 293-RRV-GFP latent cells were ~4 kb, 3 kb, and 800 nt and were similar to those of transcripts previously reported to be expressed during RRV lytic replication in RhFs (14).

To identify the transcription start site for R-LANA, we performed 5′ RACE with a primer that was antisense to the R-LANA open reading frame (Fig. 2C). Using RNA extracted from either RRV-infected RhFs at 72 h postinfection or the latently infected 293-RRV cell line, we were able to amplify two PCR products that represented transcription initiation sites, one in greater abundance than the other. Four clones were selected for sequencing the smaller, more abundant product, and all four showed a consistent transcription start site at nt 120742. Five clones from the larger, less abundant product were sequenced, and four showed a second transcription start site at nt 122201 (Fig. 2C). In the latently infected 293-RRV-GFP cell line, we found an alternate transcription initiation site at nt 120728, which was represented by the sequencing of six clones. On the 3′ end of these messages, we detected two transcription termination sites, one at nt 118197 and one at 117835. While we are currently exploring further downstream 3′ sequences using additional primers, these preliminary results confirm our observation that sense-specific R-LANA mRNAs are expressed during RRV latency as well as the lytic cycle (14).

Characterization of the R-LANA protein. Following detection of the R-LANA transcript from both lytic and latent RRV cell culture systems, we amplified by PCR and cloned the R-LANA gene with an N-terminal FLAG epitope tag into the pEF mammalian expression vector to generate a pEF–R-

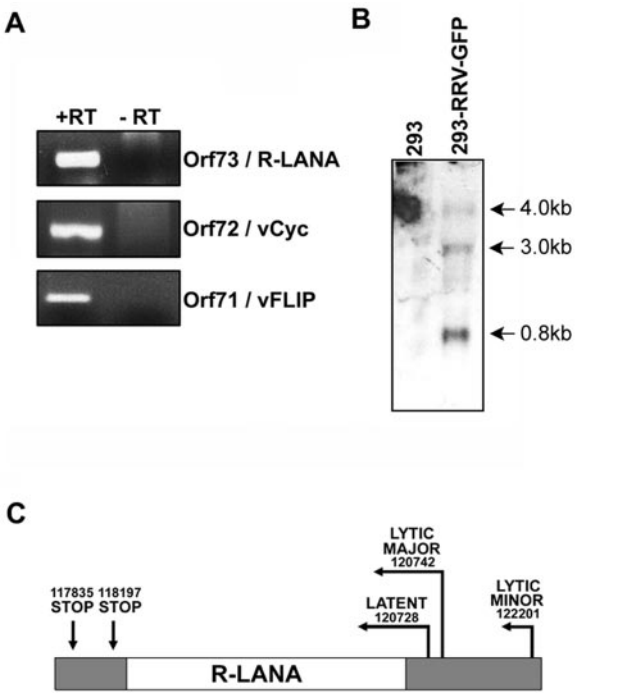

FIG. 2. R-LANA is expressed in cell lines latently infected with RRV. (A) Total RNA was harvested from latently infected 293-RRV-GFP cells, and RT-PCR was performed with primers specific for Orf71/vFLIP, Orf72/vCyc, and Orf73/R-LANA. Lanes –RT and +RT, RT-negative and -positive lanes, respectively. (B) Five micrograms of total RNA from either 293 or 293-RRV-GFP cells was run on an agarose gel and transferred to nitrocellulose. Northern hybridization was performed with an R-LANA ^{32}P-labeled DNA probe. Three bands were observed (arrows) at ~4 kB, ~3 kB, and ~800 nt. (C) 5′ RACE was used to determine the major lytic (nt 120742), minor lytic (nt 122201), and latent (nt 120728) R-LANA transcription start sites in the RRV 26–95 genome and to confirm the presence of sense-specific R-LANA transcripts in both latently infected and lytic cells. Transcription stop sites were located at nt 117835 and 118197. The start codon of R-LANA in RRV26-95 is at position 119992, and the stop codon lies at position 118646.

$LANA_{FLAG}$ plasmid. 293 cells were transfected with the pEF vector alone or the pEF–R-$LANA_{FLAG}$ plasmid. Forty-eight hours posttransfection, cells were harvested and lysed. Cell extracts were subjected to SDS-PAGE and transferred to nitrocellulose. Immunoblotting was performed with FLAG antibody (Sigma). We observed that the R-LANA protein migrated as a doublet at a molecular mass of approximately 70 kDa, as shown in Fig. 3A, which is higher than its predicted molecular mass of 49 kDa. The appearance of a doublet suggested the possibility that R-LANA was phosphorylated within the cell. To test this idea, we performed immunoprecipitations on 293 cells transiently transfected with the pEF-R-$LANA_{FLAG}$ plasmid and subjected the immunoprecipitated protein to CIP treatment. We observed that the presence of CIP shifted all of the R-LANA-specific signal to the faster-migrating form, which we interpret to represent the hypophosphorylated protein (Fig. 3B). This experiment suggests that R-LANA is phosphorylated similarly to KSHV LANA.

KSHV LANA has been shown to multimerize into a higher-order structure, and this homodimerization appears to be important for its function (55). To determine if R-LANA pos-

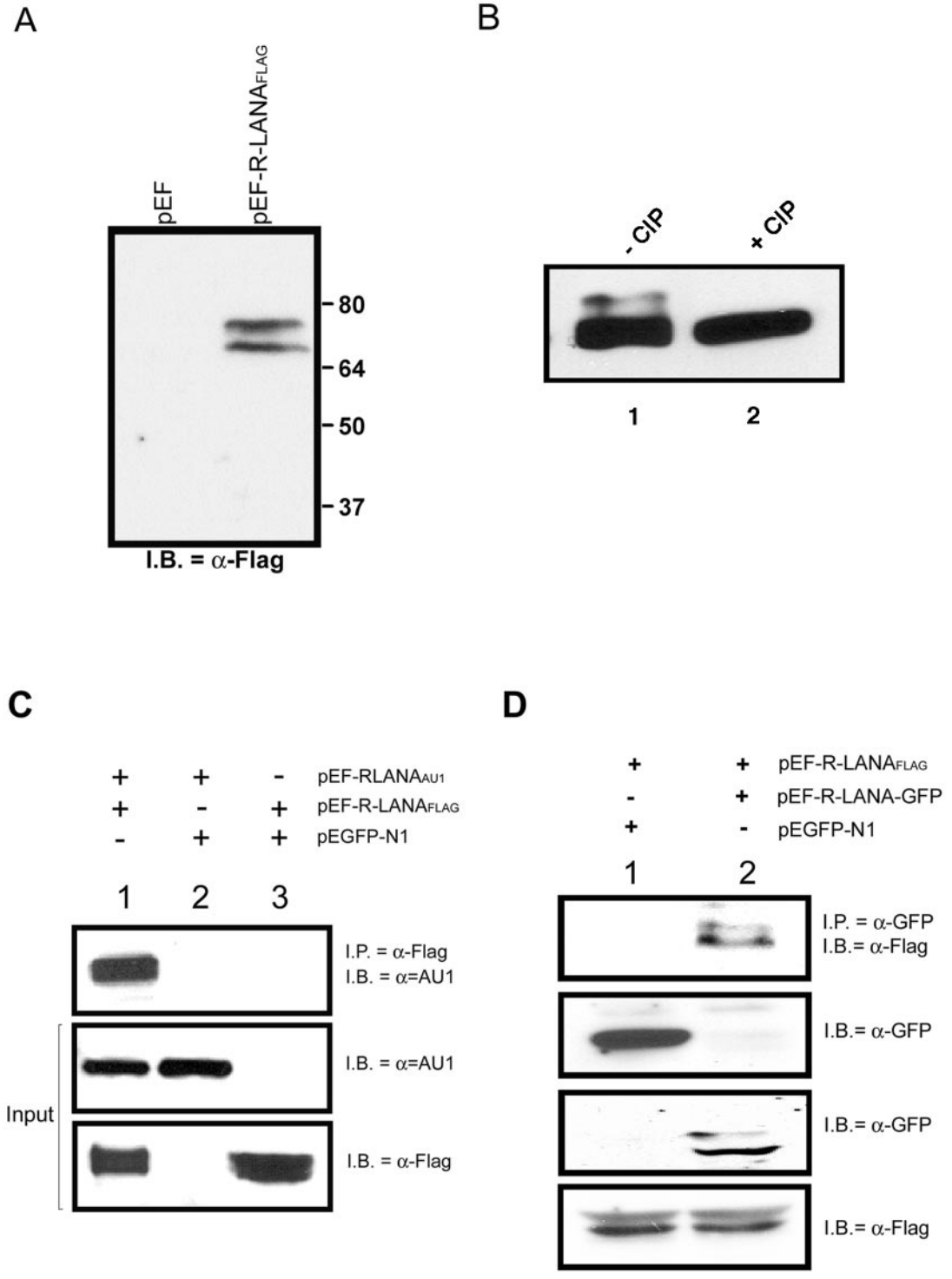

FIG. 3. The R-LANA protein can form homodimers. (A) R-LANA mobility by SDS-PAGE. Ten-centimeter dishes of 293 cells were transfected with either 15 μg of the pEF empty vector or the pEF-R-LANA$_{FLAG}$ plasmid, and cells were harvested 48 h posttransfection. Lysates were subjected to SDS-PAGE. Western blotting was performed with an anti-FLAG (α-FLAG) antibody, and R-LANA-specific bands were visualized at approximately 70 kDa. I.B., immunoblotting. (B) R-LANA is a phosphorylated protein. Immunoprecipitated R-LANA$_{FLAG}$ from three 10-cm dishes of 293 cells transfected with the pEF-R-LANA$_{FLAG}$ plasmid was divided equally and digested with CIP (lane 1) or mock digested (lane 2) and subjected to Western blotting with an anti-FLAG antibody. (C) R-LANA can undergo homodimerization. 293 cells on 10-cm dishes were transfected with 10 μg of either pEF-R-LANA$_{AU1}$, pEF-R-LANA$_{FLAG}$, or pEGFP-N1, as indicated. Lysates were immunoprecipitated (I.P.) with an anti-FLAG monoclonal antibody, washed stringently, and subjected to SDS-PAGE. Western blotting was performed with an anti-AU1 antibody. (D) R-LANA dimerizes with itself but does not bind GFP. 293 cells on 10-cm dishes were transfected with 10 μg of pEF-R-LANA$_{FLAG}$ and either 10 μg of pR-LANA-GFP or 10 μg of pEGFP-N1, as indicated. Lysates were immunoprecipitated with an anti-GFP monoclonal antibody, washed stringently, and subjected to SDS-PAGE. Western blotting was performed with either an anti-FLAG antibody or an anti-GFP antibody.

sesses a similar capacity to multimerize, we transfected different combinations of plasmids expressing an N-terminal AU1 epitope-tagged R-LANA protein (pEF-R- $LANA_{AU1}$), a FLAG epitope-tagged R-LANA protein (pEF-R-$LANA_{FLAG}$), or pEGFP-N1, which expresses GFP, into 293 cells. Forty-eight hours later, cells were harvested and lysed, and immunoprecipitations were performed with either a FLAG (Sigma) or AU1 (Covance) antibody. Immunoprecipitates were subjected to SDS-PAGE, and Western blotting was performed with the reciprocal antibody. As shown in Fig. 3C, when the $R\text{-}LANA_{FLAG}$ and $R\text{-}LANA_{AU1}$ proteins were coexpressed in 293 cells, an immunoprecipitation with the anti-FLAG antibody pulled down the $R\text{-}LANA_{AU1}$ protein (lane 1, top). However there was no detectable $R\text{-}LANA_{AU1}$ protein seen when either the $R\text{-}LANA_{AU1}$ protein or the $R\text{-}LANA_{FLAG}$ protein was individually coexpressed with GFP (Fig. 3C, top, lanes 2 and 3, respectively). Protein expression from each of the transfected expression plasmids was confirmed by Western blotting (Fig. 3C, middle and bottom). To confirm that R-LANA does indeed homodimerize, we also performed cotransfections of $R\text{-}LANA_{FLAG}$ with either enhanced GFP or R-LANA–GFP. Cells were harvested and lysed 48 h posttransfection and subjected to immunoprecipitations as described above. The immunoprecipitates were subjected to SDS-PAGE and Western blot analysis with anti-GFP and anti-FLAG antibodies (Fig. 3D). $R\text{-}LANA_{FLAG}$ immunoprecipitated with R-LANA–GFP but not with the GFP protein itself (Fig. 3D). These findings provide further confirmation that the R-LANA protein can undergo homodimerization.

R-LANA exhibits a punctate nuclear staining pattern. To determine the subcellular localization of R-LANA, we designed a fusion construct, $R\text{-}LANA_{FL}$–RFP, consisting of the full-length (FL) R-LANA protein fused in-frame to the amino terminus of RFP (Fig. 4a). To delineate the domains of R-LANA that were responsible for its cellular localization, several mutant R-LANA proteins were also constructed and fused in-frame to the dsRed protein, as depicted in Fig. 4a. Specifically, $R\text{-}LANA_{1–25}$–RFP represents a protein with the first 25 amino acids of R-LANA fused to the N terminus of RFP. Similarly, $R\text{-}LANA_{46–448}$–RFP and $R\text{-}LANA_{297–448}$–RFP represent proteins with amino acids 46 to 448 and amino acids 297 to 448 of R-LANA, respectively, fused to RFP. Plasmids expressing the full-length R-LANA protein ($R\text{-}LANA_{FL}$–RFP), $R\text{-}LANA_{1–25}$–RFP, $R\text{-}LANA_{46–448}$–RFP, and $R\text{-}LANA_{297–448}$–RFP were individually transfected into RhFs. Forty-eight hours posttransfection, cells were fixed and treated with DAPI stain and visualized under a fluorescence microscope.

As shown in Fig. 4b, panel A, full-length R-LANA ($R\text{-}LANA_{FL}$–RFP) exhibited a nuclear speckled staining pattern, much like that described for its KSHV homolog (29, 47). The $R\text{-}LANA_{FLAG}$ protein also exhibited a similar nuclear speckled localization (data not shown), and hence we conclude that the RFP fusion did not alter the localization of R-LANA. The first 25 amino acids of R-LANA ($R\text{-}LANA_{1–25}$–RFP) are sufficient for this nuclear targeting and the punctate localization of the protein, as depicted in Fig. 4b, panel B. Other fusion proteins representing the first 302, 159, and 75 amino acids showed the same localization (data not shown). A fusion construct lacking the first 45 amino acids ($R\text{-}LANA_{46–448}$–RFP) also showed a predominately nuclear distribution (Fig. 4b, panel C), implying the presence of a C-terminal nuclear localization sequence as well. However, the marked punctate distribution pattern seen with the full-length and $R\text{-}LANA_{1–25}$–RFP mutant proteins (Fig. 4b, panels A and B) was lost in the C-terminal-spanning $R\text{-}LANA_{46–448}$–RFP mutant protein, demonstrating that the N-terminal 25 amino acids are necessary and sufficient for the punctate localization pattern of full-length R-LANA. Interestingly, when only the C terminus of the fusion protein was expressed, specifically amino acids 297 to 448 ($R\text{-}LANA_{297-448}$–RFP), the protein was localized to the nucleus in two punctate spots, reminiscent of a nucleolar staining pattern (Fig. 4b, panel D). To further investigate this possibility and to determine if full-length R-LANA was also targeted to the nucleolus, we cotransfected R-LANA–RFP with a fibrillarin-GFP fusion construct (19), previously described to have a nucleolar localization. Our data indicate that the full-length R-LANA protein and the $R\text{-}LANA_{297-448}$ mutant protein (Fig. 4c) partially localize to the nucleolus since expression of R-LANA–RFP and $R\text{-}LANA_{297-448}$–RFP partially overlaps with that of fibrillarin-GFP (Fig. 4c, panels A and B, respectively). Overall, these data demonstrate that R-LANA, similar to KSHV LANA, exhibits a nuclear speckled localization and appears to possess two nuclear localization sequences, at the N and C termini of the protein (29, 44, 47). However, a nucleolar distribution for KSHV LANA has never been described, and thus this may represent an RRV-specific property or a novel property of both homolog proteins.

RRV LANA binds the viral episome during latency. One of the main functions of the KSHV LANA protein is to tether the

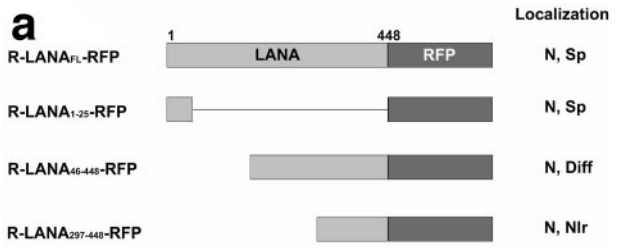

FIG. 4. Cellular localization of R-LANA. (a) Mutant R-LANA–RFP proteins. Mutant R-LANA proteins were generated by PCR, and all products were fused in-frame to the N terminus of RFP. The localization of R-LANA is denoted as follows: N, nuclear; Sp, speckled; Diff, diffuse; Nlr, nucleolar. (b) Subcellular localization of mutant R-LANA–RFP proteins. RhFs were transfected with R-LANA–RFP (A), $R\text{-}LANA_{1-25}$–RFP (B), $R\text{-}LANA_{46-448}$–RFP (C), and $R\text{-}LANA_{297-448}$–RFP (D). Forty-eight hours later, cells were fixed and stained with DAPI. Images were captured under a fluorescence microscope. For panels A through D, the upper left section shows a phase-contrast image, the upper right section shows a DAPI image, the lower left section shows RFP, and the lower right section shows an overlay of DAPI and RFP. (c) Nucleolar localization of R-LANA. RhFs were transfected with fibrillarin-GFP and R-LANA–RFP (A) or $R\text{-}LANA_{297-448}$-RFP (B). Forty-eight hours later, cells were fixed and stained with DAPI. Images were captured under a fluorescence microscope. (A) Phase-contrast image (a), green fluorescence with fibrillarin-GFP combined with DAPI staining (b), red fluorescence of the R-LANA–RFP protein combined with DAPI staining (c), and an overlay of fibrillarin-GFP, R-LANA–RFP, and DAPI staining (d). (B) Phase-contrast image (e), green fluorescence with fibrillarin-GFP combined with DAPI staining (f), red fluorescence of the $R\text{-}LANA_{297-448}$–RFP protein combined with DAPI staining (g), and an overlay of fibrillarin-GFP, $R\text{-}LANA_{297-448}$–RFP, and DAPI staining (h).

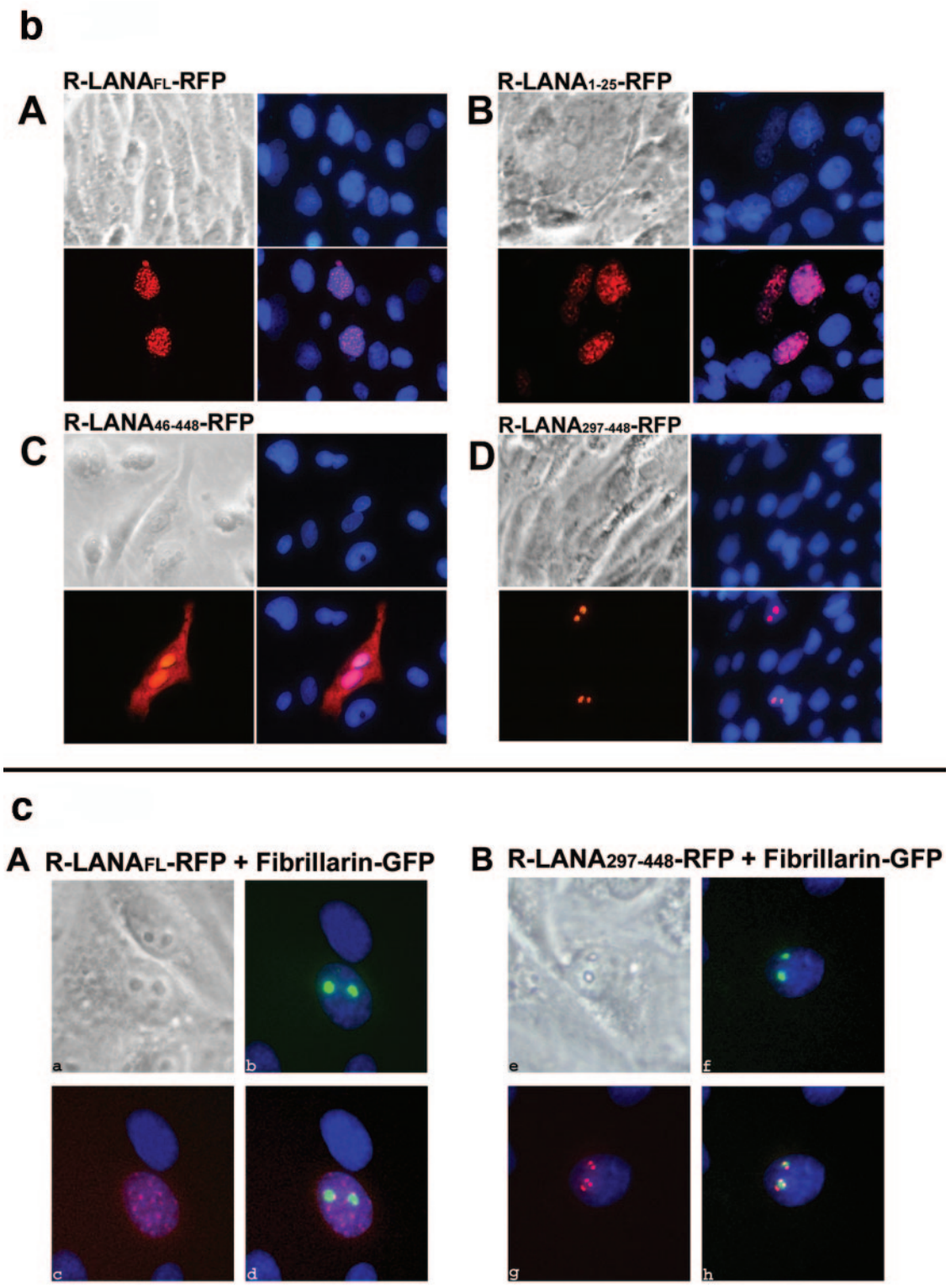

FIG. 4—*Continued.*

KSHV episome to the host cell mitotic chromosomes, in order to ensure segregation of viral genomes to daughter cells (4, 9, 10, 23, 24, 26). To determine whether R-LANA can bind the RRV genome during latency, we employed an immunoprecipitation assay. Latently infected 293-RRV-GFP cells were transfected with either a plasmid expressing RFP or the R-LANA$_{FL}$–RFP construct. Forty-eight hours later, cells were harvested, lysed, and then subjected to immunoprecipitation

with an anti-RFP antibody. Immunoprecipitates were subjected to several stringent washes, and DNA was eluted from the beads with a sodium bicarbonate-SDS buffer and subjected to a dot blot hybridization procedure. DNA immunoprecipitated by the RFP and R-LANA$_{FL}$–RFP proteins was spotted on nitrocellulose, along with known quantities of RRV-GFP genomic DNA, and the membrane was probed with ^{32}P-labeled GFP DNA (Fig. 5A). The intensity signals of the hybridized probes were quantitated with a Molecular Dynamics PhosphorImager (Fig. 5B). We observed that the R-LANA–RFP fusion protein bound more RRV genomic DNA than the RFP protein alone. We also repeated this immunoprecipitation assay using lysates from 293-RRV-GFP cells transfected with either the pEF-R-LANA$_{FLAG}$ or pEF plasmid alone, performed an immunoprecipitation reaction with the anti-FLAG antibody, and subjected the immunoprecipitated DNA to a more sensitive real-time PCR assay (15) in order to quantitate the amount of viral genomes bound by R-LANA. Using this assay, we found that R-LANA bound the RRV genome to a significantly greater extent (eightfold) than the pEF empty vector alone. Because the immunoprecipitation technique that we employed does not involve sonication or shearing of the DNA, we think it likely that the viral genome is maintained as an extrachromosomal episome, as would be the case for true herpesviral latency. These results indicate that, similar to its KSHV homolog, R-LANA, can bind the viral genome during RRV latency.

RRV LANA overexpression inhibits viral replication in vitro. We previously reported that R-LANA is transcribed during the RRV lytic cycle (14). To understand the role of R-LANA during RRV replication, we infected RhFs with RRV in the presence of exogenously expressed R-LANA. RhFs on 10-cm dishes were transiently transfected with 20 μg of pEF vector alone or pEF-R-LANA$_{FLAG}$. Twenty-four hours posttransfection, the cells were infected with RRV-GFP at an MOI of ≥1. Seventy-two hours postinfection, viral supernatant was harvested and quantitated by a previously established real-time PCR assay (15). We observed that R-LANA expression dramatically inhibited RRV replication in RhFs and that there was a 2.5-fold reduction in viral titer (Fig. 6). R-LANA's effects on the RRV lytic cycle, compared to its effects on RhFs expressing RFP alone, could also be reproduced in RhFs expressing the R-LANA–RFP fusion protein (data not shown), confirming that the presence of R-LANA inhibited viral replication, and this effect was not due to expression of a nonspecific exogenous protein, such as RFP. Interestingly, this reduction in viral titer also correlated with a reduced degree of cellular cytopathicity (as observed by microscopy) in the RhF cells that expressed the R-LANA–RFP protein.

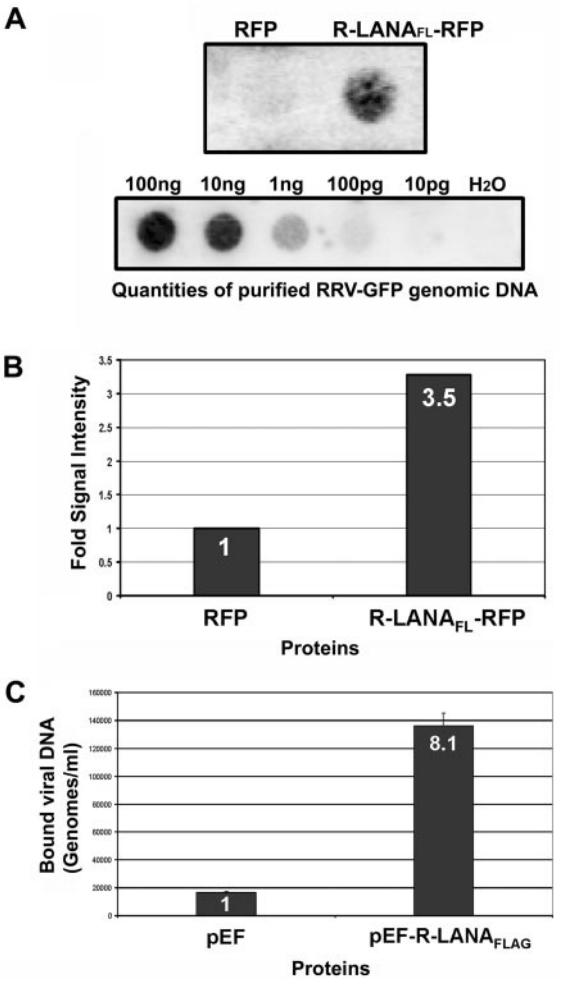

FIG. 5. R-LANA can bind the RRV viral genome. (A) Dot blot hybridization. 293-RRV-GFP cells in a 10-cm dish were transfected with 15 μg of the indicated plasmids. Seventy-two hours posttransfection, cells were lysed and immunoprecipitated with an anti-dsRed antibody. DNA was eluted from the beads and evaluated for viral DNA content by dot blot hybridization with a GFP probe. Top, DNA eluted from the anti-dsRed immunoprecipitation reactions; bottom, various quantities of RRV-GFP viral genomic DNA spotted on the same nitrocellulose filter. All hybridized spots were quantitated with a Molecular Dynamics PhosphorImager. (B) The signal intensity of RRV viral DNA bound to the full-length R-LANA$_{FL}$–RFP fusion protein was 3.5 times greater than the intensity of DNA bound to the RFP alone. (C) 293 cells were transfected and harvested as described for panel A. Lysates were immunoprecipitated with an anti-FLAG antibody. DNA was eluted from the beads and evaluated for viral DNA content with a sensitive real-time PCR assay. An approximately eightfold-greater amount of RRV genomic DNA was bound to the R-LANA protein than to the vector control.

RRV LANA interferes with Orf50 transactivation of lytic promoters. We have previously reported that RRV Orf50 can activate the RRV Orf50 (Orf50p), R8 (R8p), and Orf57 (Orf57p) promoters (14). Direct repression of these RRV lytic promoters by R-LANA is one mechanism that could explain how R-LANA inhibits lytic replication. To test this idea, we transfected the Or50p, R8p, and Orf57p luciferase reporter constructs (14), along with either the pEF empty vector or pEF-R-LANA$_{FLAG}$, into 293 cells. Cells were harvested 48 h posttransfection, and cell lysates were subjected to a luciferase assay. All luciferase activities were normalized to the vector alone. Normalized luciferase activity in the presence of Orf50 was set at 100%, and the luciferase activities of other samples were calculated as percentages of Orf50 activity. R-LANA expression alone did not significantly affect the transcriptional activity of any of these promoters either positively or negatively, i.e., R-LANA could not activate or inhibit transcription above or below that of the basal transcriptional level (Fig. 7). However, when equal amounts of pEF-R-LANA and pcDNA3-RRV Orf50 expression plasmids (2.5 μg each) were

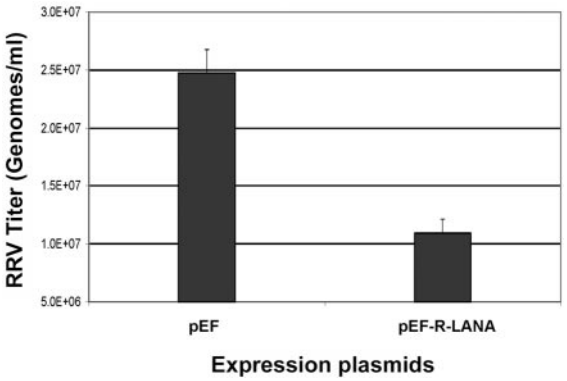

FIG. 6. R-LANA inhibits RRV lytic replication. RhFs were transfected with either pEF or pEF-R-LANA$_{FLAG}$. Twenty-four hours posttransfection, the cells were subsequently infected with RRV-GFP at an MOI of ≥1. Seventy-two hours postinfection, cell-free supernatants were harvested and assayed for viral DNA by real-time PCR.

cotransfected into 293 cells with the Orf50p, R8p, and Orf57p reporter constructs, R-LANA could markedly downregulate RRV Orf50's ability to activate these three promoters by 33 to 61% compared to the vector control (Fig. 7). Hence, it appears likely that this general interference of Orf50's transactivation function may account for R-LANA's inhibition of lytic replication.

R-LANA's repression of RRV Orf50 transactivation is mediated through HDACs. To determine the specific mechanism of R-LANA's interference of Orf50 function, we explored the possibility that histone deacetylase complexes (HDACs) played a role in inhibition. In KSHV, Orf50 has been shown to interact with HDAC1 (25), and LANA has also been implicated in histone deacetylation by its association with mSIN3

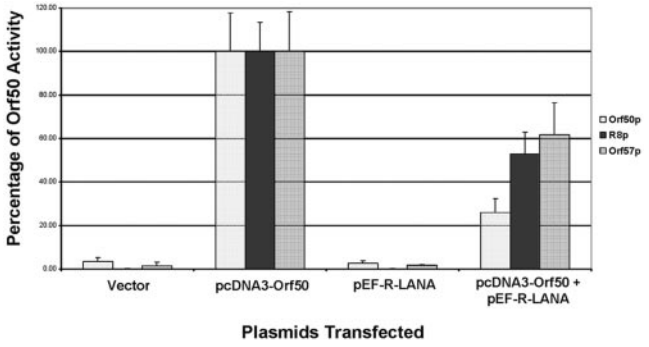

FIG. 7. R-LANA interferes with RRV Orf50 transactivation. 293 cells were transfected with 0.5 μg of the indicated reporter and 2.5 μg of each of the expression plasmids. The vector samples received 2.5 μg of pcDNA3 and 2.5 μg of pEF. The Orf50 samples received 2.5 μg of pcDNA3-Orf50 and 2.5 μg of pEF. The R-LANA samples received 2.5 μg of pcDNA3 and 2.5 μg of pEF-R-LANA. The Orf50-plus-R-LANA samples received 2.5 μg of pcDNA3-ORF50 plus 2.5 μg of pEF-R-LANA. The three lytic RRV promoter-reporter constructs, Orf50p, R8p, and Orf57p, have been previously described (14). Cells were harvested 48 h posttransfection, and lysates were assayed for luciferase activity. Luciferase activity for cells transfected with each of the individual promoter-reporter constructs (Orf50p, R8p, and Orf57p) and pcDNA3-Orf50 alone was assigned a value of 100%. The luciferase activities of the other samples were then calculated as percentages of the activity obtained with pcDNA3-Orf50 alone.

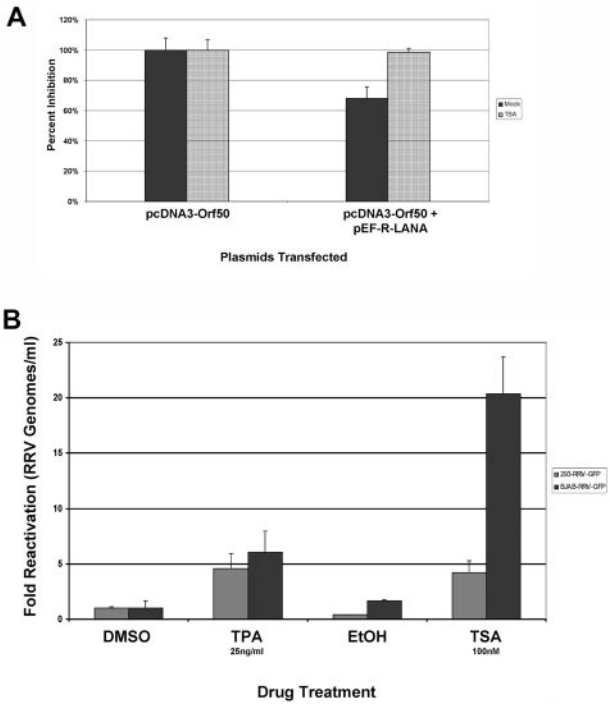

FIG. 8. TSA relieves R-LANA-mediated repression and promotes viral reactivation. (A) 293 cells were transfected with the indicated plasmids and treated with either TSA (gray bars) or ethanol (black bars). Luciferase activities for cells transfected with pcDNA3-Orf50 alone were set at 100%, and luciferase activities of the cells cotransfected with pcDNA3-Orf50 and pcDNA3-R-LANA were calculated as percentages of the activity seen with RRV Orf50 alone. (B) The 293-RRV-GFP (gray bars) and BJAB-RRV-GFP (black bars) cell lines were treated with either TPA (25 ng/ml) or an equivalent volume of DMSO and TSA (100 nM) or an equivalent volume of ethanol. Seventy-two hours postinduction, cell-free supernatants were harvested and viral titers were analyzed by a RRV real-time PCR assay.

(33). We cotransfected 293 cells with the RRV Orf50p reporter and the pcDNA3-Orf50 and pEF-R-LANA expression plasmids (Fig. 8A). The HDAC inhibitor TSA or vehicle (ethanol) was added to the cells 30 h posttransfection at a concentration of 100 nM. We observed that the presence of TSA severely compromised R-LANA's repressive properties and that R-LANA could no longer interfere with Orf50 transactivation of the Orf50p construct (Fig. 8A). These data have been normalized with full Orf50 activity set at 100% to show the differences more clearly. As can be seen in Fig. 8A, the activity of the Orf50p reporter in the presence of RRV Orf50, R-LANA, and TSA was 99% of the activity seen with RRV Orf50 alone. In contrast, in the presence of R-LANA, RRV Orf50, and the mock ethanol control, the activity of the same Orf50p-luciferase reporter was 66% of the activity seen with RRV Orf50 alone (Fig. 8A), which is consistent with the level of inhibition seen in previous assays. Importantly, when these promoters were transfected with Orf50 alone in the absence of R-LANA and treated with TSA, their activation was 90.3% of that seen with the identical TSA-treated samples (data not shown). This suggests that TSA can relieve R-LANA-mediated transcriptional repression and that this is not a consequence of

TSA increasing the general transcriptional activity of Orf50 on these promoters.

Because TSA relieved R-LANA-mediated repression of the Orf50 promoter, we next determined the biological consequence of this effect by testing whether TSA could induce viral reactivation in cells latently infected with RRV. BJAB-RRV-GFP and 293-RRV-GFP cells were treated with either TPA, DMSO, TSA, or ethanol for 72 h, and cell-free supernatants were harvested to assay for the presence of RRV by real-time PCR (15). As shown in Fig. 8B, TSA treatment produced more viral genomes in the supernatant of latently infected cells than did treatment with vehicle (ethanol) alone, suggesting that TSA relieves R-LANA repression and induces viral reactivation (Fig. 8B). We also observed that TSA was a more effective activator of BJAB-RRV-GFP cells than TPA, by a margin of approximately fourfold (Fig. 8B). Further, in a dose-response experiment, we noted that increasing concentrations of TSA up to 2 μM were even more powerful inducers of RRV reactivation from BJAB-RRV-GFP cells, with 10-fold more virus being produced than with TPA (data not shown). Furthermore, sodium butyrate, another HDAC inhibitor, was able to marginally induce reactivation in the BJAB-RRV-GFP cells, but not to the same extent as TSA (data not shown).

DISCUSSION

In this report, we describe, for the first time, the characterization and functional properties of RRV LANA. We have also created two cell lines that latently harbor RRV, which will provide useful tools to study RRV latency and reactivation. One of these cell lines, BJAB-RRV-GFP is of B-cell origin, a cell type previously shown to be a major site of persistent infection in rhesus macaques infected with RRV (6). These two cell lines are capable of reactivation to undergo lytic replication by TPA or TSA. These cell lines can also be reactivated with *n*-butyrate or by transfection of RRV Orf50 (data not shown).

Northern hybridization of total RNA from either BJAB-RRV-GFP or 293-RRV-GFP cells indicated that R-LANA is transcribed during latent RRV infection. Previously, we have reported that messages for sense-specific R-LANA transcripts are produced during lytic infection (14). In this report, the same pattern and size of R-LANA-encoded transcripts were observed in the latent-RRV-infected cells. Further, we also observed mRNA transcripts specific for ORFs 71 and 72, the viral FLIP, and cyclin D1 homologs by RT-PCR in the latently infected cells. These polycistronic transcripts encoding RRV LANA, v-cyclin, and vFLIP are similar to those described for KSHV (17, 52).

The R-LANA protein migrated as a doublet at a molecular mass of ~70 kDa. This doublet was reduced to a single band upon treatment with CIP, which demonstrated that R-LANA is phosphorylated. The phosphorylated form of the protein appears to be the less abundant of the two protein species. The functional significance of R-LANA phosphorylation or the kinase responsible for R-LANA phosphorylation is currently unknown. However, since R-LANA phosphorylation occurs in RRV-negative cell lines, we can speculate that the kinase involved in this phosphorylation is not likely to be of viral origin.

We determined that, similar to its KSHV counterpart (4, 9, 10, 23, 24, 26, 36), R-LANA could also bind the RRV viral genome, and we are currently mapping the exact RRV genomic region that interacts with R-LANA. R-LANA exhibited a speckled nuclear subcellular localization when expressed as an RFP fusion protein. This localization pattern is identical to that observed for KSHV LANA in BCBL-1 cells (29, 47). The region of R-LANA responsible for this localization lies within the first 25 amino acids of the protein. This is equivalent to the position identified as the host chromosome binding site for KSHV LANA (44). Further mutational analysis of this region in KSHV LANA revealed that three stretches within amino acids 5 to 13 are necessary (5), specifically $_{5}$GMR$_{7}$, $_{8}$LRS$_{10}$, and $_{11}$GRS$_{13}$. R-LANA contains three similar motifs within amino acids 3 to 19, specifically $_{3}$GSR$_{5}$, $_{16}$GLR$_{18}$, and $_{17}$LRS$_{19}$, any of which may regulate the observed localization and subsequent binding to the rhesus chromosome.

We also found that R-LANA has multiple nuclear localization signals. In addition, the C-terminal 151 amino acids demonstrated a nucleolar localization, as evidenced by their colocalization with fibrillarin-GFP. This is an interesting result because the full-length protein does not show the same intense subnuclear localization. This suggests that full-length R-LANA contains a motif capable of nucleolar localization or interaction with a nucleolar protein that is likely regulated or masked by another region of the R-LANA protein. Other herpesviral proteins, such as the Marek's disease virus MEQ oncoprotein, have been shown to be localized to the nucleolus (38), and this property is governed by amino acids rich in arginine and lysine. R-LANA has two stretches of arginine and lysine residues (RKYRPQRR and KKARRR) in its carboxy terminus that could potentially mediate this localization, and studies to identify the sequences responsible for this nucleolar localization are ongoing.

Exogenous expression of R-LANA in RhFs dramatically inhibited RRV replication, resulting in a 2.5-fold reduction in viral titer at 72 h postinfection. We observed that cells expressing the R-LANA–RFP fusion protein, when infected with our RRV-GFP recombinant virus, were more resistant to virus-induced cytopathicity. The green fluorescence of the RRV-GFP virus in these cells was dimmer than that in neighboring cells not expressing R-LANA–RFP (S. M. DeWire and B. Damania, unpublished observation), thus suggesting a lower viral copy number in R-LANA-expressing RhFs. These subjective findings lend support to the results that we obtained from our quantitative real-time PCR assays showing that R-LANA expression in RhFs decreased RRV viral titers. Using this type of analysis, we cannot rule out the possibility that R-LANA is indirectly causing some cellular toxicity or altering cellular stress response pathways. However, the abundance of data that we present here regarding the direct impact of R-LANA on the transcriptional regulation of the Orf50 promoter suggests that this is a significant mechanism that contributes to the inhibition of RRV replication by R-LANA. Similar analyses have been used in other related viral systems. For example, in herpesvirus saimiri (HVS), the same inhibition of de novo lytic replication by Orf73 has been observed (52). In HVS, Orf73's ability to directly repress the lytic switch gene promoter is the mechanism used to explain the inhibition of lytic replication observed with this protein (53). While we did not observe any direct effect of R-LANA expression on the RRV

Orf50 promoter in the absence of the RRV Orf50 protein, it is possible that the RRV Orf50 promoter fragment used in our assay (which contains a 193-nt element upstream of the Orf50 transcription start site (14), may be too minimal and that a larger RRV Orf50p fragment may be more susceptible to R-LANA-mediated repression. While this article was in preparation, Lan et al. (35) reported that KSHV LANA can inhibit KSHV viral reactivation by interaction with Orf50 (58). However this report did not address the mechanism for how KSHV LANA can mediate the repression of Orf50 function. Our findings suggest that the mechanism of R-LANA-mediated repression of RRV viral replication is, at least in part, mediated by activation or recruitment of HDACs. KSHV LANA has previously been shown to function as a repressor (55), and this repression appeared to be mediated through the mSiN3 complex (33). Thus, it appears that the ability to repress promoters is conserved among the LANA homologs of the gamma-herpesviruses.

One possible explanation for our finding is that R-LANA is able to posttranslationally modify or downregulate Orf50 function. We performed Western blotting on Orf50 in the presence or absence of R-LANA and found no evidence for such posttranslation changes to Orf50 (S. M. DeWire and B. Damania, unpublished observation). Another possible explanation involves chromatin remodeling. Histone acetylation and deacetylation have been implicated in KSHV Orf50 and LANA function in previous reports. Both KSHV Orf50 and LANA have been shown to interact with the histone acetyltransferase CBP (25, 37), and Orf50 has been shown to interact with HDAC1 (25). Further, histone modifications at the KSHV Orf50 promoter have been shown to result in reactivation (39). Specifically, HDAC1, -5, and -7 were associated with the KSHV Orf50 promoter, and upon treatment with HDAC inhibitors were replaced by CBP, resulting in transcription (39). Because the addition of TSA abolished R-LANA-mediated interference of RRV Orf50 and induced RRV reactivation from the latently infected 293-RRV-GFP and BJAB-RRV-GFP cells, we speculate that a similar histone modification process likely occurs during RRV viral replication and reactivation. We cannot, however, rule out the possibility that TSA could affect other pathways that result in viral reactivation. Interestingly, KSHV has previously been reported to reactivate upon treatment with another HDAC inhibitor, *n*-butyrate (42), and this may occur through the relief of KSHV LANA-mediated repression of KSHV Orf50 function, similar to our findings with RRV LANA.

In this report, we describe the nuclear, speckled localization of R-LANA, its ability to self-associate, and its capacity to bind the latent RRV episome. We have also shown that R-LANA functions to downregulate Orf50 transcriptional activation via a mechanism that involves HDACs. Finally, we observed that R-LANA can inhibit RRV replication and we suggest that this repressive effect of R-LANA may be important in maintaining viral latency and suppressing viral reactivation. Thus, R-LANA's downregulation of RRV Orf50 function may be an evolutionarily conserved mechanism by which gamma-herpesviruses are able to suppress viral reactivation at inopportune times.

ACKNOWLEDGMENTS

We are grateful to R. Desrosiers for RRV strain H26-95 and to Mark Olson for providing us with the fibrillarin-GFP plasmid. We also thank R. E. DeWire for technical contributions and members of the Damania lab for informative discussions and manuscript reading.

S. M. DeWire is supported, in part, by American Heart Association predoctoral fellowship 0315389U. This work was supported by grants from the American Association for Cancer Research, American Heart Association (0355852U), and NIH grants CA096500 and AI58093.

REFERENCES

1. **Alexander, L., L. Denenkamp, A. Knapp, M. Auerbach, S. Czajak, B. Damania, and R. C. Desrosiers.** 1999. The primary sequence of rhesus rhadinovirus isolate 26–95: sequence similarities to Kaposi's sarcoma herpesvirus and rhesus rhadinovirus isolate 17577. J. Virol. **74:**3388–3398.
2. **An, J., A. K. Lichtenstein, G. Brent, and M. B. Rettig.** 2002. The Kaposi sarcoma-associated herpesvirus (KSHV) induces cellular interleukin 6 expression: role of the KSHV latency-associated nuclear antigen and the AP1 response element. Blood **99:**649–654.
3. **An, J., Y. Sun, and M. B. Rettig.** 2004. Transcriptional coactivation of c-Jun by the KSHV-encoded LANA. Blood **103:**222–228.
4. **Ballestas, M. E., P. A. Chatis, and K. M. Kaye.** 1999. Efficient persistence of extrachromosomal KSHV DNA mediated by latency-associated nuclear antigen. Science **284:**641–644.
5. **Barbera, A. J., M. E. Ballestas, and K. M. Kaye.** 2004. The Kaposi's sarcoma-associated herpesvirus latency-associated nuclear antigen 1 N terminus is essential for chromosome association, DNA replication, and episome persistence. J. Virol. **78:**294–301.
6. **Bergquam, E. P., N. Avery, S. M. Shiigi, M. K. Axthelm, and S. W. Wong.** 1999. Rhesus rhadinovirus establishes a latent infection in B lymphocytes in vivo. J. Virol. **73:**7874–7876.
7. **Cesarman, E., Y. Chang, P. S. Moore, J. W. Said, and D. M. Knowles.** 1995. Kaposi's sarcoma-associated herpesvirus-like DNA sequences in AIDS-related body-cavity-based lymphomas. N. Engl. J. Med. **332:**1186–1191.
8. **Chang, Y., E. Cesarman, M. S. Pessin, F. Lee, J. Culpepper, D. M. Knowles, and P. S. Moore.** 1994. Identification of herpesvirus-like DNA sequences in AIDS-associated Kaposi's sarcoma. Science **266:**1865–1869.
9. **Cotter, M. A., II, and E. S. Robertson.** 1999. The latency-associated nuclear antigen tethers the Kaposi's sarcoma-associated herpesvirus genome to host chromosomes in body cavity-based lymphoma cells. Virology **264:**254–264.
10. **Cotter, M. A., II, C. Subramanian, and E. S. Robertson.** 2001. The Kaposi's sarcoma-associated herpesvirus latency-associated nuclear antigen binds to specific sequences at the left end of the viral genome through its carboxy-terminus. Virology **291:**241–259.
11. **Damania, B., and R. C. Desrosiers.** 2001. Simian homologues of human herpesvirus 8. Philos. Trans. R. Soc. Lond. B Biol. Sci. **356:**535–543.
12. **Damania, B., J. H. Jeong, B. S. Bowser, S. M. DeWire, M. R. Staudt, and D. P. Dittmer.** 2004. Comparison of the Rta/Orf50 transactivator proteins of gamma-2-herpesviruses. J. Virol. **78:**5491–5499.
13. **Desrosiers, R. C., V. G. Sasseville, S. C. Czajak, X. Zhang, K. G. Mansfield, A. Kaur, R. P. Johnson, A. A. Lackner, and J. U. Jung.** 1997. A herpesvirus of rhesus monkeys related to the human Kaposi's sarcoma-associated herpesvirus. J. Virol. **71:**9764–9769.
14. **DeWire, S. M., M. A. McVoy, and B. Damania.** 2002. Kinetics of expression of rhesus monkey rhadinovirus (RRV) and identification and characterization of a polycistronic transcript encoding the RRV Orf50/Rta, RRV R8, and R8.1 genes. J. Virol. **76:**9819–9831.
15. **DeWire, S. M., E. S. Money, S. P. Krall, and B. Damania.** 2003. Rhesus monkey rhadinovirus (RRV): construction of a RRV-GFP recombinant virus and development of assays to assess viral replication. Virology **312:**122–134.
16. **Dezube, B. J., M. Zambela, D. R. Sage, J. F. Wang, and J. D. Fingeroth.** 2002. Characterization of Kaposi sarcoma-associated herpesvirus/human herpesvirus-8 infection of human vascular endothelial cells: early events. Blood **100:**888–896.
17. **Dittmer, D., M. Lagunoff, R. Renne, K. Staskus, A. Haase, and D. Ganem.** 1998. A cluster of latently expressed genes in Kaposi's sarcoma-associated herpesvirus. J. Virol. **72:**8309–8315.
18. **Dittmer, D., C. Stoddart, R. Renne, V. Linquist-Stepps, M. E. Moreno, C. Bare, J. M. McCune, and D. Ganem.** 1999. Experimental transmission of Kaposi's sarcoma-associated herpesvirus (KSHV/HHV-8) to SCID-hu Thy/Liv mice. J. Exp. Med. **190:**1857–1868.
19. **Dundr, M., T. Misteli, and M. O. Olson.** 2000. The dynamics of postmitotic reassembly of the nucleolus. J. Cell Biol. **150:**433–446.
20. **Fakhari, F. D., and D. P. Dittmer.** 2002. Charting latency transcripts in Kaposi's sarcoma-associated herpesvirus by whole-genome real-time quantitative PCR. J. Virol. **76:**6213–6223.
21. **Friborg, J., Jr., W. Kong, M. O. Hottiger, and G. J. Nabel.** 1999. p53 inhibition by the LANA protein of KSHV protects against cell death. Nature **402:**889–894.

22. **Fujimuro, M., and S. D. Hayward.** 2003. The latency-associated nuclear antigen of Kaposi's sarcoma-associated herpesvirus manipulates the activity of glycogen synthase kinase-3β. J. Virol. **77:**8019–8030.
23. **Garber, A. C., M. A. Shu, J. Hu, and R. Renne.** 2001. DNA binding and modulation of gene expression by the latency-associated nuclear antigen of Kaposi's sarcoma-associated herpesvirus. J. Virol. **75:**7882–7892.
24. **Grundhoff, A., and D. Ganem.** 2003. The latency-associated nuclear antigen of Kaposi's sarcoma-associated herpesvirus permits replication of terminal repeat-containing plasmids. J. Virol. **77:**2779–2783.
25. **Gwack, Y., H. Byun, S. Hwang, C. Lim, and J. Choe.** 2001. CREB-binding protein and histone deacetylase regulate the transcriptional activity of Kaposi's sarcoma-associated herpesvirus open reading frame 50. J. Virol. **75:** 1909–1917.
26. **Hu, J., A. C. Garber, and R. Renne.** 2002. The latency-associated nuclear antigen of Kaposi's sarcoma-associated herpesvirus supports latent DNA replication in dividing cells. J. Virol. **76:**11677–11687.
27. **Jenner, R. G., M. M. Alba, C. Boshoff, and P. Kellam.** 2001. Kaposi's sarcoma-associated herpesvirus latent and lytic gene expression as revealed by DNA arrays. J. Virol. **75:**891–902.
28. **Jeong, J., J. Papin, and D. Dittmer.** 2001. Differential regulation of the overlapping Kaposi's sarcoma-associated herpesvirus vGCR (orf74) and LANA (orf73) promoters. J. Virol. **75:**1798–1807.
29. **Kedes, D. H., M. Lagunoff, R. Renne, and D. Ganem.** 1997. Identification of the gene encoding the major latency-associated nuclear antigen of the Kaposi's sarcoma-associated herpesvirus. J. Clin. Investig. **100:**2606–2610.
30. **Knight, J. S., M. A. Cotter II, and E. S. Robertson.** 2001. The latency-associated nuclear antigen of Kaposi's sarcoma-associated herpesvirus transactivates the telomerase reverse transcriptase promoter. J. Biol. Chem. **276:** 22971–22978.
31. **Komatsu, T., M. E. Ballestas, A. J. Barbera, and K. M. Kaye.** 2002. The KSHV latency-associated nuclear antigen: a multifunctional protein. Front. Biosci. **7:**d726–d730.
32. **Krithivas, A., M. Fujimuro, M. Weidner, D. B. Young, and S. D. Hayward.** 2002. Protein interactions targeting the latency-associated nuclear antigen of Kaposi's sarcoma-associated herpesvirus to cell chromosomes. J. Virol. **76:** 11596–11604.
33. **Krithivas, A., D. B. Young, G. Liao, D. Greene, and S. D. Hayward.** 2000. Human herpesvirus 8 LANA interacts with proteins of the mSin3 corepressor complex and negatively regulates Epstein-Barr virus gene expression in dually infected PEL cells. J. Virol. **74:**9637–9645.
34. **Lagunoff, M., J. Bechtel, E. Venetsanakos, A. M. Roy, N. Abbey, B. Herndier, M. McMahon, and D. Ganem.** 2002. De novo infection and serial transmission of Kaposi's sarcoma-associated herpesvirus in cultured endothelial cells. J. Virol. **76:**2440–2448.
35. **Lan, K., D. A. Kuppers, S. C. Verma, and E. S. Robertson.** 2004. Kaposi's sarcoma-associated herpesvirus-encoded latency-associated nuclear antigen inhibits lytic replication by targeting Rta: a potential mechanism for virus-mediated control of latency. J. Virol. **78:**6585–6594.
36. **Lim, C., C. Choi, and J. Choe.** 2004. Mitotic chromosome-binding activity of latency-associated nuclear antigen 1 is required for DNA replication from terminal repeat sequence of Kaposi's sarcoma-associated herpesvirus. J. Virol. **78:**7248–7256.
37. **Lim, C., Y. Gwack, S. Hwang, S. Kim, and J. Choe.** 2001. The transcriptional activity of cAMP response element-binding protein-binding protein is modulated by the latency-associated nuclear antigen of Kaposi's sarcoma-associated herpes virus. J. Biol. Chem. *2***76:**31016–31022.
38. **Liu, J. L., L. F. Lee, Y. Ye, Z. Qian, and H. J. Kung.** 1997. Nucleolar and nuclear localization properties of a herpesvirus bZIP oncoprotein, MEQ. J. Virol. **71:**3188–3196.
39. **Lu, F., J. Zhou, A. Wiedmer, K. Madden, Y. Yuan, and P. M. Lieberman.** 2003. Chromatin remodeling of the Kaposi's sarcoma-associated herpesvirus ORF50 promoter correlates with reactivation from latency. J. Virol. **77:** 11425–11435.
40. **Mansfield, K. G., S. V. Westmoreland, C. D. DeBakker, S. Czajak, A. A. Lackner, and R. C. Desrosiers.** 1999. Experimental infection of rhesus and pig-tailed macaques with macaque rhadinoviruses. J. Virol. **73:**10320–10328.
41. **Mattsson, K., C. Kiss, G. M. Platt, G. R. Simpson, E. Kashuba, G. Klein, T. F. Schulz, and L. Szekely.** 2002. Latent nuclear antigen of Kaposi's sarcoma herpesvirus/human herpesvirus-8 induces and relocates RING3 to nuclear heterochromatin regions. J. Gen. Virol. **83:**179–188.
42. **Miller, G., L. Heston, E. Grogan, L. Gradoville, M. Rigsby, R. Sun, D. Shedd, V. M. Kushnaryov, S. Grossberg, and Y. Chang.** 1997. Selective switch between latency and lytic replication of Kaposi's sarcoma herpesvirus and Epstein-Barr virus in dually infected body cavity lymphoma cells. J. Virol. **71:**314–324.
43. **Paulose-Murphy, M., N. K. Ha, C. Xiang, Y. Chen, L. Gillim, R. Yarchoan, P. Meltzer, M. Bittner, J. Trent, and S. Zeichner.** 2001. Transcription program of human herpesvirus 8 (Kaposi's sarcoma-associated herpesvirus). J. Virol. **75:**4843–4853.
44. **Piolot, T., M. Tramier, M. Coppey, J. C. Nicolas, and V. Marechal.** 2001. Close but distinct regions of human herpesvirus 8 latency-associated nuclear antigen 1 are responsible for nuclear targeting and binding to human mitotic chromosomes. J. Virol. **75:**3948–3959.
45. **Platt, G. M., G. R. Simpson, S. Mittnacht, and T. F. Schulz.** 1999. Latent nuclear antigen of Kaposi's sarcoma-associated herpesvirus interacts with RING3, a homolog of the *Drosophila* female sterile homeotic (*fsh*) gene. J. Virol. **73:**9789–9795.
46. **Radkov, S. A., P. Kellam, and C. Boshoff.** 2000. The latent nuclear antigen of Kaposi sarcoma-associated herpesvirus targets the retinoblastoma-E2F pathway and with the oncogene Hras transforms primary rat cells. Nat. Med. **6:**1121–1127.
47. **Rainbow, L., G. M. Platt, G. R. Simpson, R. Sarid, S. J. Gao, H. Stoiber, C. S. Herrington, P. S. Moore, and T. F. Schulz.** 1997. The 222- to 234-kilodalton latent nuclear protein (LNA) of Kaposi's sarcoma-associated herpesvirus (human herpesvirus 8) is encoded by *orf73* and is a component of the latency-associated nuclear antigen. J. Virol. **71:**5915–5921.
48. **Renne, R., D. Blackbourn, D. Whitby, J. Levy, and D. Ganem.** 1998. Limited transmission of Kaposi's sarcoma-associated herpesvirus in cultured cells. J. Virol. **72:**5182–5188.
49. **Renne, R., D. Dittmer, D. Kedes, K. Schmidt, R. C. Desrosiers, P. A. Luciw, and D. Ganem.** 2004. Experimental transmission of Kaposi's sarcoma-associated herpesvirus (KSHV/HHV-8) to SIV-positive and SIV-negative rhesus macaques. J. Med. Primatol. **33:**1–9.
50. **Renne, R., W. Zhong, B. Herndier, M. McGrath, N. Abbey, D. Kedes, and D. Ganem.** 1996. Lytic growth of Kaposi's sarcoma-associated herpesvirus (human herpesvirus 8) in culture. Nat. Med. **2:**342–346.
51. **Sakurada, S., H. Katano, T. Sata, H. Ohkuni, T. Watanabe, and S. Mori.** 2001. Effective human herpesvirus 8 infection of human umbilical vein endothelial cells by cell-mediated transmission. J. Virol. **75:**7717–7722.
52. **Sarid, R., O. Flore, R. A. Bohenzky, Y. Chang, and P. S. Moore.** 1998. Transcription mapping of the Kaposi's sarcoma-associated herpesvirus (human herpesvirus 8) genome in a body cavity-based lymphoma cell line (BC-1). J. Virol. **72:**1005–1012.
53. **Schafer, A., D. Lengenfelder, C. Grillhosl, C. Wieser, B. Fleckenstein, and A. Ensser.** 2003. The latency-associated nuclear antigen homolog of herpesvirus saimiri inhibits lytic virus replication. J. Virol. **77:**5911–5925.
54. **Schultz, E. R., G. W. Rankin, Jr., M. P. Blanc, B. W. Raden, C. C. Tsai, and T. M. Rose.** 2000. Characterization of two divergent lineages of macaque rhadinoviruses related to Kaposi's sarcoma-associated herpesvirus. J. Virol. **74:**4919–4928.
55. **Schwam, D. R., R. L. Luciano, S. S. Mahajan, L. Wong, and A. C. Wilson.** 2000. Carboxy terminus of human herpesvirus 8 latency-associated nuclear antigen mediates dimerization, transcriptional repression, and targeting to nuclear bodies. J. Virol. **74:**8532–8540.
56. **Searles, R. P., E. P. Bergquam, M. K. Axthelm, and S. W. Wong.** 1999. Sequence and genomic analysis of a rhesus macaque rhadinovirus with similarity to Kaposi's sarcoma-associated herpesvirus/human herpesvirus 8. J. Virol. **73:**3040–3053.
57. **Soulier, J., L. Grollet, E. Oksenhendler, P. Cacoub, D. Cazals-Hatem, P. Babinet, M. F. d'Agay, J. P. Clauvel, M. Raphael, L. Degos, et al.** 1995. Kaposi's sarcoma-associated herpesvirus-like DNA sequences in multicentric Castleman's disease. Blood **86:**1276–1280.
58. **Sun, R., S. F. Lin, L. Gradoville, Y. Yuan, F. Zhu, and G. Miller.** 1998. A viral gene that activates lytic cycle expression of Kaposi's sarcoma-associated herpesvirus. Proc. Natl. Acad. Sci. USA **95:**10866–10871.
59. **Talbot, S. J., R. A. Weiss, P. Kellam, and C. Boshoff.** 1999. Transcriptional analysis of human herpesvirus-8 open reading frames 71, 72, 73, K14, and 74 in a primary effusion lymphoma cell line. Virology **257:**84–94.
60. **Wang, L., N. Wakisaka, C. C. Tomlinson, S. M. DeWire, S. Krall, J. S. Pagano, and B. Damania.** 2004. The Kaposi's sarcoma-associated herpesvirus (KSHV/HHV-8) K1 protein induces expression of angiogenic and invasion factors. Cancer Res. **64:**2774–2781.
61. **Wong, S. W., E. P. Bergquam, R. M. Swanson, F. W. Lee, S. M. Shiigi, N. A. Avery, J. W. Fanton, and M. K. Axthelm.** 1999. Induction of B cell hyperplasia in simian immunodeficiency virus-infected rhesus macaques with the simian homologue of Kaposi's sarcoma-associated herpesvirus. J. Exp. Med. **190:**827–840.